Structure of Human Annexin A6 at the Air-Water Interface and in a Membrane-Bound State

Marcin Golczak,* Aneta Kirilenko,* Joanna Bandorowicz-Pikula,* Bernard Desbat,† and Slawomir Pikula*
*Department of Cellular Biochemistry, Nencki Institute of Experimental Biology, Warsaw, Poland; and †Laboratoire de Physicochimie Molèculaire, Unité Mixte de Recherche 5803, Université de Bordeaux I, Talence, France

ABSTRACT We postulate the existence of a pH-sensitive domain in annexin A6 (AnxA6), on the basis of our observation of pH-dependent conformational and orientation changes of this protein and its N- (AnxA6a) and C-terminal (AnxA6b) halves in the presence of lipids. Brewster angle microscopy shows that AnxA6, AnxA6a, and AnxA6b in the absence of lipids accumulate at the air-water interface and form a stable, homogeneous layer at pH below 6.0. Under these conditions polarization modulation IR absorption spectroscopy reveals significant conformational changes of AnxA6a whereas AnxA6b preserves its α-helical structure. The orientation of protein α-helices is parallel with respect to the interface. In the presence of lipids, polarization modulation IR reflection absorption spectroscopy experiments suggest that AnxA6a incorporates into the lipid/air interface, whereas AnxA6b is adsorbed under the lipid monolayer. In this case AnxA6a regains its α-helical structures. At a higher pressure of the lipid monolayer the average orientation of the α-helices of AnxA6a changes from flat to tilted by 45° with respect to normal to the membrane interface. For AnxA6b no such changes are detected, even at a high pressure of the lipid monolayer—suggesting that the putative pH-sensitive domain of AnxA6 is localized in the N-terminal half of the protein.

INTRODUCTION

Annexins belong to a family of highly conserved Ca^{2+}- and lipid-binding proteins characterized by a common property of binding to membranes in a Ca^{2+}-dependent manner (Gerke and Moss, 2002); the largest member of the family is annexin A6 (AnxA6). Although the physiological role of AnxA6 is still unknown, this protein has been implicated in the pH-regulated processes related to vesicular transport: exocytosis, endocytosis, membrane aggregation, and membrane fusion (Jackle et al., 1994; Pol et al., 1997; Grewal et al., 2000; de Diego et al., 2002). AnxA6 has been shown to be predominantly associated with membranes of late endosomes and prelysosomal compartments in NRK fibroblasts, WIF-B hepatoma, and rat kidney cells (Pons et al., 2000, 2001a; de Diego et al., 2002). AnxA6 was also co-localized with marker proteins of endocytotic membranes, such as Rab5 (Ortega et al., 1998), and with protein complexes involved in various cellular signaling pathways (Chow et al., 2000; Pons et al., 2001b).

Recently, it has been shown that some annexins may interact with membranes in a Ca^{2+}-independent manner. Although the biological relevance of such interactions is not yet clear, it was suggested that one of the factors that promote the interaction of annexins with phospholipids is low pH (Kohler et al., 1997; Binder et al., 2000; Cartailler et al., 2000; Isas et al., 2000, 2003). Therefore, changes of intracellular pH may affect the properties and function of annexins (for a review see Pikula, 2003). At mildly acidic pH AnxA6 (Golczak et al., 2001a,c), AnxA5 (Binder et al., 2000; Isas et al., 2000), and AnxB12 (Luecke et al., 1995; Isas et al., 2000, 2003; Ladokhin et al., 2002) were found to behave as integral membrane proteins and to form voltage-dependent ion channels in vitro, characterized by a low specificity for transported ions. In addition, it has been recently reported that under mildly acidic conditions AnxA2 is able to bind and aggregate phospholipid membranes and form flexible bridges allowing the invagination of membranes (Lambert et al., 2004).

Due to their evolutionarily conserved sequences, it is believed that most annexins share similar properties and are able to respond in a similar manner to changes of pH. Most of the experiments concerning the effect of pH were performed using recombinant proteins. AnxA5 and AnxA6 showed upon acidification crucial changes in hydrophobicity, due to protonation of several charged residues and structural reorganization of the molecules (Kohler et al., 1997; Beermann et al., 1998; Golczak et al., 2001b). The structural reorganization consists in significant unfolding-refolding of the annexin molecule, loss of α-helix content, and formation of new β-structures, as well as other changes (e.g., oligomerization) leading to remodeling of the molecule and perhaps to creation of ion channel activity. Therefore, changes of pH turned out to be one of the most potent factors affecting the function and structure of

Submitted December 11, 2003, and accepted for publication May 10, 2004.

Address reprint requests to Slawomir Pikula, Dept. of Cellular Biochemistry, Nencki Institute of Experimental Biology, 3 Pasteur St., 02-093 Warsaw, Poland. Tel.: 48-22-589-2347; Fax: 48-22-822-53-42; E-mail: s.pikula@nencki.gov.pl.

Abbreviations used: AnxA, mammalian annexin; AnxA6a, N-terminal half of annexin A6; AnxA6b, C-terminal half of annexin A6; BAM, Brewster angle microscopy; CD, circular dichroism; DMPE, dimyristoylphosphatidylethanolamine; DMPS, dimyristoylphosphatidyl-serine; PM-IRRAS, polarization modulation infrared reflection absorption spectroscopy; SDS-PAGE, sodium dodecyl sulfate polyacrylamide gel electrophoresis; ^{125}I-TID, 3-(trifluoromethyl)-3-(*m*-[^{125}I]iodophenyl)-diazirine.

0006-3495/04/08/1215/12 $2.00 doi: 10.1529/biophysj.103.038240

annexins; in this respect these changes are much more effective than changes in intracellular Ca^{2+} concentrations. In addition, it seems that the direct changes in the molecular structure are responsible for the pH sensitivity of annexins (existence of an intramolecular pH switch). It is postulated that the intracellular localization of annexins is related to the pH sensitivity of some of them. These proteins are often detected on the surface of cellular organelles of low inner pH (Jackle et al., 1994; Jost et al., 1997; Zeuschner et al., 2001). Whether annexins become localized also inside these organelles is not clear (Cuervo et al., 2000). Participation of some accessory proteins residing in membranes of these organelles that may transmit the low pH signal to the annexin molecule localized on the cytosol-facing membrane surface cannot be excluded (Gu and Gruenberg, 2000). On the other hand, it is likely that the ability to respond to pH changes resides within the annexin molecule. One may hypothesize that upon acidification of milieu, pH-induced changes lead to a transition from a soluble to an integral membrane protein that is accompanied by an ion channel activity (Isas et al., 2000; Golczak et al., 2001a,c). Is it possible that such a molecular mechanism is valid for different annexins? One has to consider that the three annexins studied in this respect differ significantly from one another. AnxA6 is a product of gene duplication and fusion; therefore it is the largest known annexin. Its binding and mechanism of insertion within the membrane bilayer must, therefore, be much more complicated than those for the smaller annexins AnxA5 (Wu et al., 1998; Silvestro and Axelsen, 1999; Sopkowa-De Oliveira Santos et al., 2000) and AnxB12 (Langen et al., 1998a). In addition, for AnxB12, oligomerization is postulated (Langen et al., 1998b; Luecke et al., 1995; Risse et al., 2003), but in the case of AnxA6 it is not so obvious. Unlike AnxA5, AnxA6 does not form trimers on the membrane surface (Oling et al., 2001). AnxA6 can be treated as a tandem of two 4-domain annexins, since the N- and C-terminal halves of the protein exhibit similar structural properties. Contrary to this view, there are observations suggesting that the N- and C-terminal halves of AnxA6 are different in many respects (Ishitsuka et al., 1998; Garbuglia et al., 2000; Golczak et al., 2001c). In addition, AnxA6 has a flexible linker that may affect the interactions between the two halves of the protein (Benz et al., 1996; Avila-Sakar et al., 1998, 2000).

Considering the unanswered questions on the formation of ion channel by AnxA6, we wanted to determine the molecular mechanisms of the pH-dependent membrane association of AnxA6. We tested whether both halves of the protein are equivalently involved in membrane interaction. Using biochemical and biophysical methods we show that despite the fact that both halves of AnxA6 are structurally similar, only the N-terminal half is involved in strong interaction with membranes at acidic pH. Moreover, membrane lipids seem to play an important role in the changes of structure and orientation of AnxA6 molecules. The results of BAM and PM-IRRAS investigations of AnxA6 interaction with lipids reported in contemporary articles strongly support our previous experimental data (Golczak et al., 2001b,c) and help to solve the topology of the AnxA6 molecule in a membrane-bound state. Our results support the molecular mechanism of spontaneous, post-translational incorporation of proteins into membranes proposed by White et al. (2001).

MATERIALS AND METHODS

Materials

Dimyristoylphosphatidylserine (DMPS) and dimyristoylphosphatidylethanolamine (DMPE) were purchased from Sigma-Aldrich (St. Quentin Fallavier, France); before use, these lipids were dissolved in chloroform or in a chloroform/methanol mixture (20%, v/v) at 5 mg/ml. Organic solvents were obtained from Prolabo (Nancy, France). Ultrapure water (Milli-Q, Bedford, MA) was used for all buffers and solutions. Monoclonal anti-human AnxA6 antibodies were from BD Transduction Laboratories (Lexington, KY). 3-(Trifluoromethyl)-3-(*m*-[^{125}I]iodophenyl)-diazirine (spec. ac. 10 Ci/mmol) (^{125}I-TID) was purchased from Amersham (Freiburg, Germany). All other chemicals of the highest purity available were purchased from Sigma-Aldrich (Poznan, Poland).

Preparation of recombinant human AnxA6 and its N- and C-terminal peptide fragments

Human recombinant AnxA6, as well as its N-terminal-AnxA6a (residues 2–342) and C-terminal-AnxA6b (residues 348–673) peptide fragments, were expressed in *Escherichia coli* strain Bl21(DE3) and purified as described by Burger et al. (1993) with further modifications described in details in earlier reports from our laboratory (Kirilenko et al., 2002; Bandorowicz-Pikula et al., 2003). Fractions containing the respective peptides eluted from the last ion exchange column were combined, dialyzed against 5 mM Tris-HCl, pH 7.4, and lyophilized and stored at −20°C until use. The purity and concentration of proteins was examined by silver-staining of SDS-PAGE gels and by the Bradford method (Bradford, 1976) with bovine serum albumin as a standard, respectively.

Proteolytic digestion of AnxA6

AnxA6 or its peptide fragments (20 μg of protein) were incubated with liposomes made of asolectin in 20 mM citrate buffer, pH 5.0, 100 mM NaCl, 0.1 mM EGTA, 0.2 M sucrose for 30 min at room temperature. The molecular ratio of protein to lipids was kept at 1:1000. The digestion was initiated by adding 5 μg of pepsin and carried on at 37°C for 1–2 h. Aliquots of the reaction mixture (15 μl) were collected at various time intervals to prepare electrophoretic samples; the digestion was stopped by increasing the pH with 1 μl of 1 M KOH per sample. The peptide composition of the samples was examined by SDS-PAGE.

Labeling of AnxA6 and its N- and C-terminal fragments with ^{125}I-TID

AnxA6 or its peptide fragments (15 μg) were incubated with lipid vesicles (1:100 molar ratio) preincubated in darkness with 1 μCi of ^{125}I-TID for 30 min. The total sample volume was fixed at 30 μl. To keep the pH constant, 30 mM Tris-HCl, pH 7.4 or 20 mM citrate buffer, pH 3.0–6.2, were used. Additionally, the samples contained 100 mM NaCl and 0.1 mM EGTA (at pH 3.0–6.2) or 1 mM $CaCl_2$ (at pH 7.4). After incubation for 20 min the

samples were subjected to UV light irradiation using a handheld UV lamp (UVGL-58, Ultra-Violet Products, San Gabriel, CA) for 20 min at a distance of 5 cm. Then, SDS-PAGE sample buffer was added and peptides were separated from the liposomes by SDS-PAGE. The resulting gels were exposed to medical x-ray film (Foton, Warsaw, Poland) for 5–14 days.

Langmuir setup and surface pressure measurements

Changes in the surface pressure (π) of the air/buffer interface and of lipid monolayers induced by AnxA6 were investigated using a NIMA tensiometer (Nima Technology, Coventry, UK). The experiments were performed in a Teflon trough (70 cm^3) using Whatman Ch1 paper strips of a fixed area and known wetness (Whatman, Maidstone, Kent, UK). The aqueous subphase was 10 mM HEPES, pH 7.4, 2 mM Ca^{2+}, 150 mM NaCl, or 20 mM citrate buffer, pH 5.0, containing 0.1 mM EGTA and 50 or 150 mM NaCl. Proteins were added from concentrated stock solutions to the subphase to a final concentration of 300 nM. Phospholipid monolayers (DMPS/DMPE, 1:1 mol/mol) were formed by spreading a few microliters of a 5 mg/ml lipid solution in chloroform on the subphase until a desired pressure was reached. To investigate protein interaction with the lipid monolayer, AnxA6 or its peptide fragments were injected into the subphase and the pressure change ($\Delta\pi$) in time was continuously recorded, digitized, and stored by using the computer software provided by the equipment manufacturer. All measurements were performed at room temperature.

Brewster angle microscopy

Using a Brewster angle microscope (NFT BAM2plus, Göttingen, Germany) the morphology of AnxA6 molecules at the air-water interface or those interacting with phospholipid monolayers was investigated. The BAM-derived contrast within a film originates from the difference in reflectivity to *p*-polarized light incident at the Brewster angle for pure air-water interface (Kaercher et al., 1993–1994). Under our experimental conditions, the air-water or lipid monolayer/water interface was illuminated at $\theta \approx 53.1°$ by a helium-neon laser beam ($\lambda = 532$ nm, 20 mW) polarized in the plane of incidence (*p*-polarized), and the reflected light was collected by a lens system focusing the image onto a charge-coupled device camera. Images from the camera were recorded and analyzed directly by computer software. The gray level of pictures is linearly proportional to the reflectance of interfacial structures to *p*-polarized light. Each reported value of gray-scale represents the mean of a Gaussian fit to a gray-scale histogram taken from one image. Pictures shown in this report (see Fig. 6) were collected at a spatial resolution of 2 μm and are representatives of at least three reproducible experiments. The image size corresponds to 650 $\times$ 400 μm. Estimation of the thickness of the lipid and protein layers was done using the software provided by the BAM setup producer.

PM-IRRAS measurements

The conformation and orientation of AnxA6 molecules at the air-water interface as well as in interaction with lipids was determined in situ by PM-IRRAS. PM-IRRAS measurements were performed using a Nicolet 740 spectrometer equipped with a HgCdTe detector cooled with liquid nitrogen (Thermo Electron, Nicolet Instrument, Madison, WI). An infrared beam was conducted out of the spectrometer and focused onto the same Teflon trough as used for tensiometric measurements and equipped with the Nima surface pressure detector. The optimal angle of incidence was 75° to the interface normal. The incident beam line was polarized by a ZnSe polarizer and modulated by a ZnSe modulator between parallel (*p*) and perpendicular (*s*) polarization. The principles of PM-IRRAS and the experimental setup are described in details in Blaudez et al. (1996). At least 400 scans were collected for each spectrum at a resolution of 8 cm^{-1}. The spectra were treated using OMNIC software version 5.1 (Nicolet Instrument, 1992–1999). To remove the contribution of water absorption, each spectrum was divided by a corresponding spectrum of the subphase buffer containing no further additions.

For experiments made only with proteins (in the absence of lipids), solution of AnxA6 or its peptide fragments was injected into the subphase to reach a final concentration of 300 nM. For protein-lipid mixtures, first the phospholipids were spread until a desired surface pressure was reached. After chloroform evaporation, spectrum of pure lipids was taken as a reference and then the protein solution was added to the subphase.

Circular dichroism measurements

Far-UV (range 190–260 nm) CD spectra of proteins were collected at 25°C using an AVIV CD spectrophotometer (AVIV Associates, Lakewood, NJ) in a 2-mm optical pathlength quartz cell. The assay media contained 10 mM citrate buffer, pH 3.0–6.2 and 0.1 mM EGTA. Protein concentration was fixed at 0.1 mg/ml.

Miscellaneous methods

Sodium dodecyl sulfate polyacrylamide gel electrophoresis (SDS-PAGE, under reducing conditions) was performed on 5% stacking and 12% resolving gels; the gels were stained with Coomassie brilliant blue (Laemmli, 1970). Western blotting was performed according to Towbin et al. (1979). Liposomes were prepared in the presence of 0.25 M sucrose from asolectin, as described by Reeves and Dowben (1969).

RESULTS

AnxA6 adsorption at the air-water interface induced by acidic pH

To investigate pH-dependent changes in AnxA6 surface properties experiments were performed in neutral and acidic pH. At pH 7.4, even in the presence of 2 mM $CaCl_2$, AnxA6, as well as its N- and C-terminal peptide fragments, did not localize at the air-water interface, as reflected by very small changes of surface pressure, ~1–2 mN/m (not shown). In contrast, at pH 5.0 AnxA6 significantly increased the interface pressure, at a subnanomolar concentration range of the protein (Fig. 1). The maximal lateral pressure of protein layer (exceeding 14 mN/m) was reached at 300 nM AnxA6. The peptide fragment AnxA6a had properties similar to those of the intact protein whereas AnxA6b used at the same concentration evoked changes in surface pressure at least two-times weaker than AnxA6. The time dependence of the lateral pressure changes after injection of AnxA6 or its fragments into the subphase are presented in Fig. 1. The formation of an AnxA6 layer at the air-water interface as indicated by the increase of lateral pressure can be explained by an increase in the hydrophobicity of AnxA6 molecules upon acidification (Golczak et al., 2001b). Furthermore, the differences in the hydrophobicity of the N- and C-terminal peptide fragments of AnxA6 could be responsible for the observed variance of lateral pressures between the two peptides upon formation of a protein layer at the air-water interface.

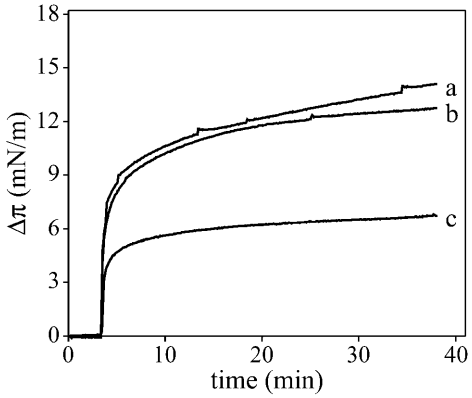

FIGURE 1 Kinetics of the lateral pressure surface tension (π) increases of the air-water interface in the presence of AnxA6 or its fragments. The subphase contained 20 mM citrate buffer, pH 5.0, 100 mM NaCl, and 0.1 mM EGTA. AnxA6 (*trace a*) or its N- (*trace b*) and C-terminal (*trace c*) fragments were added to a final concentration of 300 nM. One representative trace of at least three experiments is shown. The experiments varied by <5%.

Structure of AnxA6 at the air-water interface in the absence of lipids

The ability of AnxA6 molecules to form a stable layer at the air-water interface at pH 5.0 allowed us to investigate possible changes in protein conformation and orientation caused by buffer acidification and increased surface pressure.

The PM-IRRAS spectra of AnxA6 (Fig. 2 *A*) exhibit a strong positive amide-I band located at 1655 cm^{-1} which corresponds mostly to the peptide backbone carbonyl stretching mode and to a small extent to the C-N stretching mode. A weaker amide-II band with the maximum at 1544 cm^{-1} is also observed corresponding to peptide backbone C-N stretching and C-N-H bending modes. The strong band located at 1655 cm^{-1} is characteristic for α-helix, suggesting that even at an acidic pH the secondary structure of AnxA6 remains mostly α-helical. The band shape of the amide-I region reveals β-sheet structures, as shown earlier by a comparison of infrared spectra of porcine AnxA6 collected at neutral and acidic pH (Golczak et al., 2001a). β-Sheet structures produce band-splitting of the amide-I band at ~1628 cm^{-1} (shoulder) and a faint component band at 1680–1677 cm^{-1}. The existence of a random coil within AnxA6 structure is suggested by the presence of a band located at 1644 cm^{-1}. The shape of the amide-I band is stable in time and does not change with protein concentration. The evidence for a conformational transition of AnxA6 at low pH in solution, characterized by partial unfolding, collected using PM-IRRAS, is in excellent agreement with the results of CD measurements obtained previously (Golczak et al., 2001b,c). With increasing surface pressure the intensities of both bands were augmented, but no significant changes in band shapes were observed. This suggests that the spectral changes were caused by an increasing amount of AnxA6 at the air-water interface, consistent with the augmentation of surface pressure.

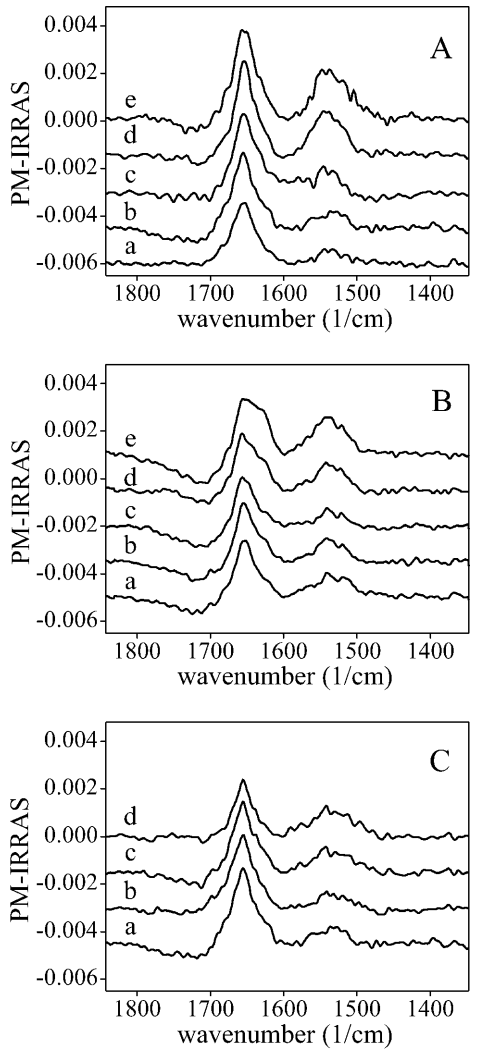

FIGURE 2 PM-IRRAS spectra of AnxA6 (*A*) and its N- (*B*) or C-terminal (*C*) fragments at the air-water interface. Spectra were collected at the different surface pressures of the protein monolayer: 3 mN/m (*traces a*), 6 mN/m (*traces b*), 9 mN/m (*traces c*), 14 mN/m (*traces d*), and 20 mN/m (*traces e*). The subphase contained 20 mM citrate buffer, pH 5.0, 100 mM NaCl, and 0.1 mM EGTA. Bulk protein concentration was 300 nM. One set of representative spectra of four independent experiments performed at the same conditions is shown. The experiments varied by <5%.

In the case of AnxA6a all the spectra displayed an amide-I band at ~1657 cm^{-1} and amide-II band centered at ~1540 cm^{-1} (Fig. 2 *B*). At increased surface pressure, the band shapes of the amide-I region changed significantly. This is especially the case for the presence of β-sheets (as evidenced by the bands located at 1627 and 1696 cm^{-1}, better seen at a high surface pressure). The component band characteristic for α-helices was observed at 1657 cm^{-1} and for random coils at 1646 cm^{-1}. The intensity of the bands corresponding to β-sheets in the spectra of AnxA6a is much higher than observed for AnxA6, indicating either a higher content of β-sheets or changes in the orientation of β-sheet structures. This reveals a dramatic change in the secondary structure of the N-terminal part of the

protein as a function of time and protein concentration. In contrast, no significant conformational transitions of the C-terminal part of AnxA6 (Fig. 2 *C*) were observed upon acidification. The main amide-I band is located at 1655 cm^{-1}. The lower intensity of the AnxA6b PM-IRRAS signal is probably due to the fact that surface properties of AnxA6b (its concentration at the air-water interface) are weaker than those of the N-terminal peptide fragment and full length AnxA6.

Spatial orientation of AnxA6 molecules at the air-water interface

The possibility of orientation changes with increasing concentration of AnxA6 at the air-water interface was examined by analyzing the PM-IRRAS spectra of the protein at different surface pressures. The ratio of amide-I/amide-II absorbances was taken as a measure of relative orientation changes of protein molecules. The previously reported simulations of the relative intensity of amide-I band for pure α-helices (Blaudez et al., 1996) revealed that spectra dominated by a single positive band with a maximum near 1650 cm^{-1} corresponded to helices oriented at a tilt angle of 90° with respect to the plane of the air-water interface (Lavoie et al., 1999; Castano et al., 2002). The simulated spectra suggested that with a lower tilt angle the positive amide-I band diminished in intensity and a negative peak occurred at a slightly higher wavenumber (Lavoie et al., 1999). All the spectra presented in Fig. 2 *A* exhibit a strong positive amide-I band ~1650 cm^{-1}, and a medium amide-II band, suggesting an orientation of the α-helices parallel to or slightly tilted with respect to the interface.

Structure of AnxA6 in solution at low pH

The differences in the response to low pH observed in the PM-IRRAS spectra of the N- and C-terminal peptide fragments of AnxA6 were confirmed by measuring CD spectra of these peptides. In the case of AnxA6a the spectra reveal that lowering the pH of the assay medium results in a drop of α-helix content (changes in the intensity of the characteristic minima at 209 and 222 nm) and an increase of β-structures as well as appearance of some unordered structures (Fig. 3 *A*). It is worth mentioning that despite the partial unfolding of the protein it still contains a significant amount of α-helix within its structure. For AnxA6b no significant structural changes were observed upon acidification (Fig. 3 *B*). The above-described dependence of AnxA6a structure on pH is in perfect agreement with the results obtained for intact AnxA6 (Golczak et al., 2001a,c). Moreover, behavior of both peptide fragments in solution suggests their independent folding.

Interaction of AnxA6 with lipid monolayers

Penetration of AnxA6 or its peptide fragments into phospholipid monolayers was followed by measurement of the surface pressure changes at a constant area. A fixed amount of AnxA6 or its peptide fragments was injected under lipid monolayers condensed to the initial surface pressure of 27 mN/m. The typical curves of $\Delta\pi$ versus time reveal that the overall pressure changes for AnxA6 and its N-terminal peptide fragment AnxA6a (Fig. 4, *trace a* and *trace b*) are much higher than for AnxA6b (Fig. 4, *trace c*). After AnxA6 or AnxA6a injection the surface pressure further increases up to 7 mN/m in $<$1 h. AnxA6b at the same concentration caused only a slight increase of monolayer pressure, not higher than 1 mN/m in 1 h.

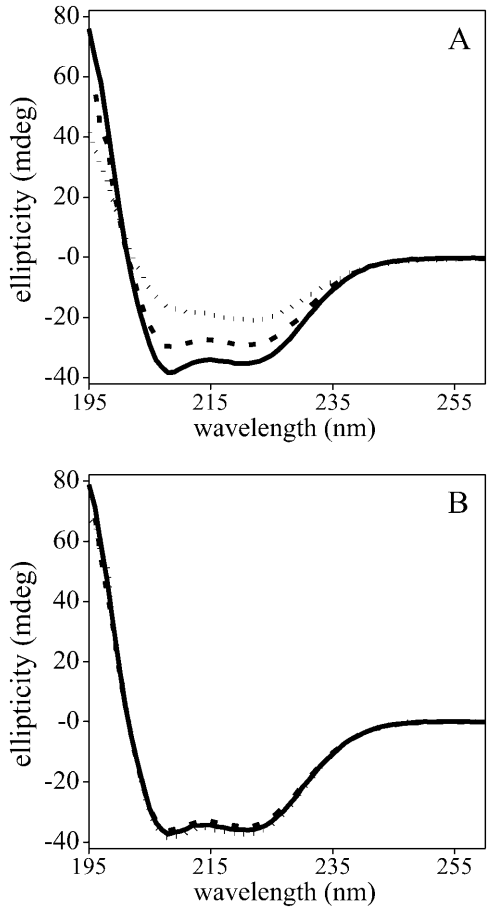

FIGURE 3 Far-UV CD spectra of AnxA6a (*A*) and AnxA6b (*B*). Solid line corresponds to the spectra collected at pH 7.5, dashed line represents pH 6.2 and short-dashed one pH 4.6. To maintain pH values, 10 mM citrate buffer was used, which in addition contained 0.1 mM EGTA. The assay medium of total volume 0.6 ml contained 0.24 mg of AnxA6a or AnxA6b. All measurements were performed at 25°C using a 2-mm optical pathlength cuvette.

Proteolytic digestion of membrane-bound AnxA6

To define the nature of the differences in the lipid-binding properties of the N- and C-terminal peptide fragments of AnxA6 and the topology of incorporation of AnxA6a into

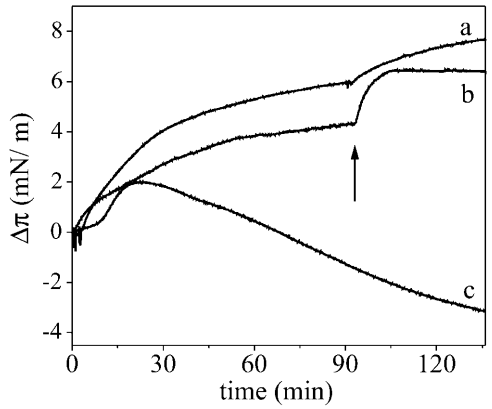

FIGURE 4 The effect of AnxA6 or its peptide fragments on the surface pressure of a lipid monolayer. The lipid monolayer was made from DMPS:DMPE mixed at a weight ratio of 1:1. The subphase contained 20 mM citrate buffer, pH 5.0, 100 mM NaCl, and 0.1 mM EGTA. After stabilization on the initial surface pressure of the lipid monolayer at 27 mN/m, the proteins were added in two equal aliquots (at time zero and as indicated by *arrow*) to reach the final protein concentration of 300 nM. Further additions did not produce any significant effects or even resulted in lipid monolayer collapse. The traces are marked as follows: trace *a*, AnxA6; trace *b*, AnxA6a; and trace *c*, AnxA6b. They represent typical traces chosen from at least three independent experiments performed under the same conditions.

the hydrophobic core of the lipid membrane at low pH, controlled proteolysis of AnxA6 and its fragments in the presence of liposomes was performed (Fig. 5). Digestion of AnxA6 in the presence of liposomes gives a proteolytic fragment of ~30 kDa. The 30-kDa fragment is protected from digestion on prolonged proteolysis (Fig. 5 *A*, *lanes 2* and *4*). In the absence of liposomes, AnxA6 is digested to smaller fragments already after 1 h (Fig. 5 *A*, *lanes 3* and *5*). To identify the origin of the 30-kDa fragment the same experiment was performed with AnxA6a and AnxA6b (Fig. 5 *B*). In the presence of liposomes AnxA6a is not completely digested, giving a fragment of 30 kDa whereas the C-terminal peptide (AnxA6b) completely vanishes (Fig. 5 *B*, *lanes 1–3*). The 30-kDa proteolytic fragment of AnxA6 was further identified using monoclonal antibodies against the N-terminal half of AnxA6. After 1 h of proteolysis the composition of peptides remaining in the sample was examined by Western blotting (Fig. 5 *C*). The resistant fragment of AnxA6 was recognized by the antibodies. The observed protection from digestion may suggest that the N-terminal part of AnxA6 inserts into the hydrophobic region of the membrane, therefore becoming inaccessible for the soluble proteases.

Labeling of AnxA6 with ^{125}I-TID

Other evidence for the insertion of the N-terminal portion of AnxA6 molecule into the hydrophobic core of lipid membranes upon acidification is provided by labeling of

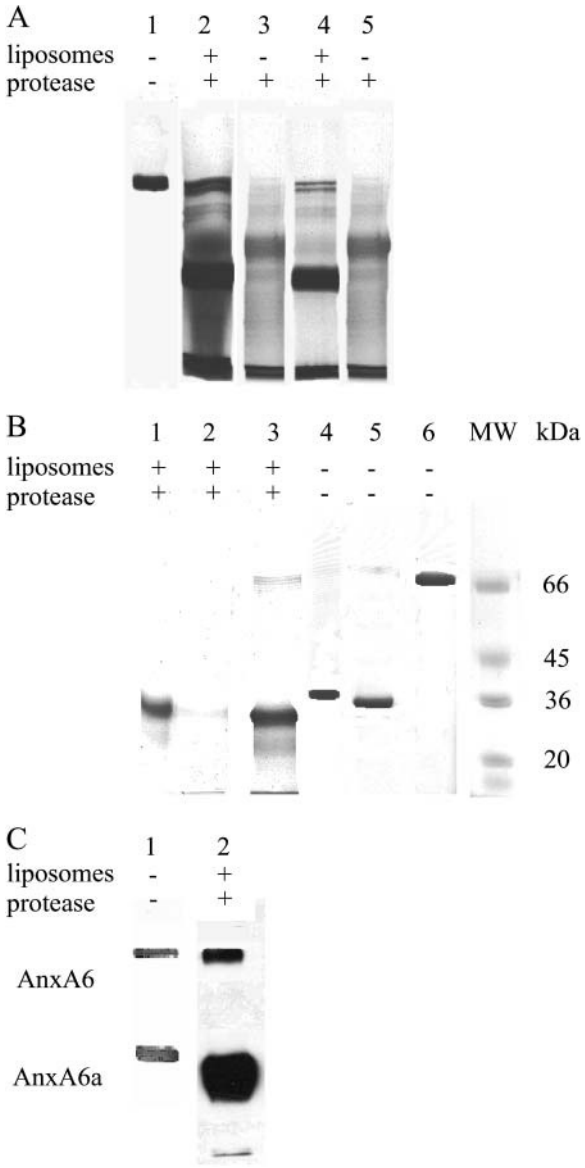

FIGURE 5 Proteolytic digestion of AnxA6 or its peptide fragments in the presence of liposomes at low pH. The reaction was performed in total volume of 40 μl containing 20 mM citrate buffer, pH 5.0, 100 mM NaCl, 0.1 mM EGTA, and 40 μg of protein. Proteolysis was initiated by adding 5 μg of pepsin and terminated by alkalization of the reaction medium by adding 1 μl of 1 M KOH. Then the products of proteolysis were separated by SDS-PAGE. (*A*) Digestion of AnxA6. Lane *1*, standard of AnxA6 (nondigested protein); lanes *2* and *4* show the digestion products formed in the presence of liposomes (+) after 1 and 2 h of digestion, respectively; and lanes *3* and *5*, digestion of AnxA6 in the absence of lipids (−) for 1 and 2 h, respectively. (*B*) The same experiment performed using the N- and C-terminal peptide fragments of AnxA6. Lanes *1–3* represent products of proteolysis of AnxA6a, AnxA6b, and AnxA6, respectively, in the presence of liposomes (+) for 1 h; lanes *4–6* show corresponding nondigested proteins used in the experiment. *MW*, molecular weight standards. (*C*) Identification of the products of controlled proteolysis by Western blotting. Lane *1*, standards of AnxA6 and its N-terminal fragment AnxA6a; lane *2*, products of proteolysis of AnxA6 for 1 h in the presence of liposomes (+), recognized by monoclonal antibodies against the N-terminal part of AnxA6.

AnxA6 molecules with ^{125}I-TID, a hydrophobic reagent that selectively binds protein domains exposed to the hydrophobic core of membranes (Hoppe et al., 1984; van Voorst et al., 1998). As one could expect, due to surface binding of AnxA6 to the membrane at pH 7.4, in the presence of Ca^{2+} AnxA6 is not labeled with ^{125}I-TID (Fig. 6, *upper row*). In contrast, the protein binds ^{125}I-TID at a pH below 6.0, indicating that it inserts in the hydrophobic core of the membrane. Consistent with the observed differences between the two peptide fragments of AnxA6, only the N-terminal AnxA6a exhibits similar properties as the whole protein, being labeled with ^{125}I-TID in the presence of liposomes at acidic pH (Fig. 6, *middle row*). The C-terminal peptide fragment was never labeled with ^{125}I-TID under our experimental conditions, suggesting that AnxA6b does not significantly penetrate the core region of the lipid bilayer (Fig. 6, *lowest row*). In the control experiments, in the absence of liposomes AnxA6 and its peptide fragments did not bind ^{125}I-TID (data not shown). Additionally, in the presence of lipids a soluble protein, calmodulin, did not bind ^{125}I-TID either (data not shown).

Morphology of AnxA6 interacting with lipid monolayer

BAM images taken as a function of time after injection of AnxA6 or its peptide fragments beneath DMPS/DMPE monolayer at pH 5.0 are shown in Fig. 7, *A–C*. On increasing the surface pressure the average normalized gray level and the luminosity progressively increased from GL 50, OS 120 up to GL 100, OS 500, the initial small white spots slowly disappeared upon AnxA6 adsorption and the final state displayed a homogenous phase of very high luminosity, which allowed us to estimate the thickness of the mixed protein-lipid layer by using the ''Multicouche'' software (Buffeteau et al., 1999). Using refractive indexes of $n = 1.45$ for lipids and $n = 1.50$ for proteins and fixing the thickness of the lipids at 20 Å the estimated thickness of the protein amounted to 26 Å for AnxA6, 18 Å for the N-terminal peptide fragment and 12 Å for AnxA6b. The

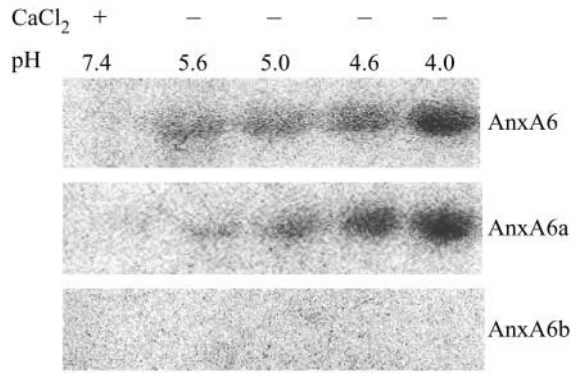

FIGURE 6 Labeling of AnxA6 and its N- or C-terminal peptide fragments with ^{125}I-TID. The autoradiogram shown is characteristic for three independent experiments. Proteins were incubated with vesicles containing ^{125}I-TID at indicated pH in the presence of Ca^{2+} (+) or EGTA (−). After exposition to UV light (for 20 min) samples were separated from unbound reagent by SDS-PAGE. The gels were then exposed to x-ray film. Analysis of the autoradiograms revealed that except for the presented bands and low molecular weight material at the dye front of the gel, no other radioactive material was detected.

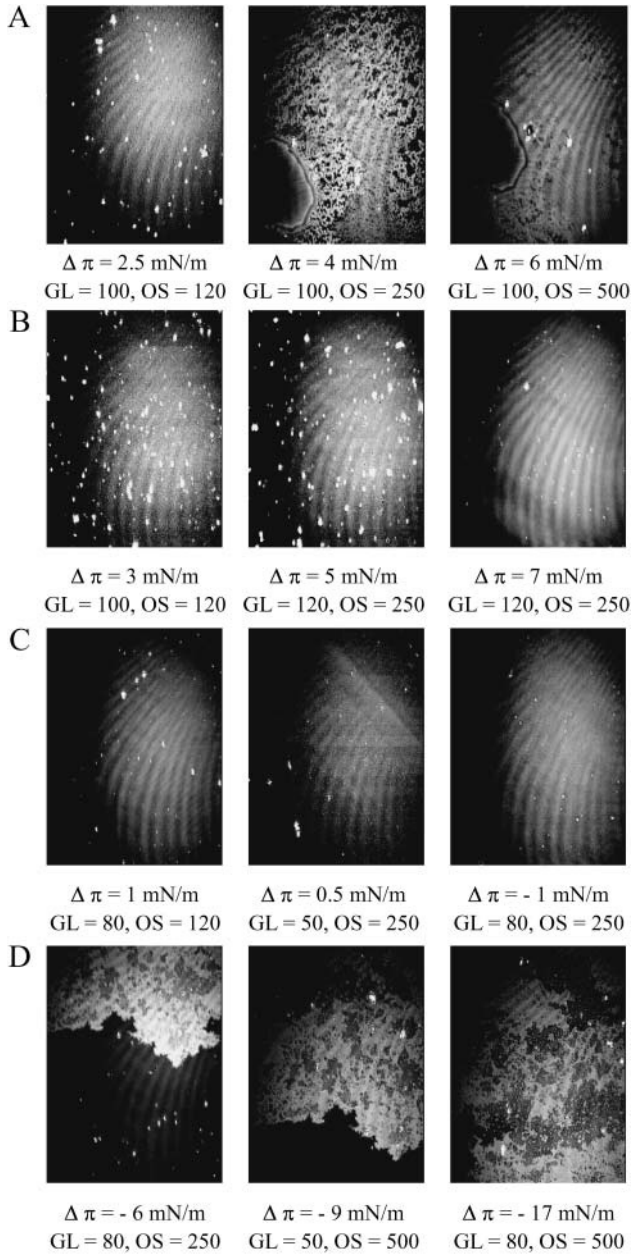

FIGURE 7 BAM images of lipid monolayers made of DMPS:DMPE (at a weight ratio of 1:1) recorded after addition of AnxA6 (*A*), AnxA6a (*B*), or AnxA6b (*C*) into the subphase consisting of 20 mM citrate buffer, pH 5.0, 100 mM NaCl, and 0.1 mM EGTA. Reference gray level (*GL*) was 25 at shutting time (*OS*) 50; protein concentration was 300 nM. The real image size is 625 × 500 μm. (*D*) The same experiment performed with AnxA6 at pH 7.4 (20 mM Tris-HCl buffer, 100 mM NaCl) in the presence of 1 mM $CaCl_2$.

above calculation is an estimation but it suggests that only single monolayer of AnxA6 is adsorbed under the lipid monolayer. Moreover, the difference in thickness between the halves of AnxA6 is an evidence for differences in α-helix orientation. One has to remember that the BAM technique also reflects changes in optical properties that fluctuate with time. The proteins attached to the lipid monolayer formed a fluid film as judged by its motion in the BAM instrument.

The morphology of the AnxA6 protein monolayer at neutral pH in the presence of Ca^{2+} (Fig. 7 *D*) reveals striking differences from that at low pH. The first bright spots appear later than in the case of low pH. After ~2 h, the surface of the lipid film is fully covered with protein molecules and the mixed protein/lipid film becomes more rigid and condensed.

Structure and orientation of AnxA6 in membrane-bound state

To investigate the behavior of AnxA6 in interaction with lipid monolayers, PM-IRRAS spectra of AnxA6 and DMPE:DMPS (1:1) monolayer were collected at the initial phospholipid pressure fixed at 25 mN/m. In the spectra of pure phospholipids several characteristic bands can be identified (Fig. 8 *A*, *dotted line*). The band located at 1730 cm^{-1} corresponds to the stretching of ester bonds, the band ~1460 cm^{-1} represents the scissoring mode of the methylenes (δ CH_2) of the lipid acyl chains, and the broad 1240 cm^{-1} band is assigned to antisymmetric P=O stretching vibration (Blaudez et al., 1996).

Penetration of AnxA6 molecules into the condensed lipid monolayer led to the appearance of amide-I and amide-II bands located at 1652 and 1548 cm^{-1}, respectively. Subtraction of the pure lipid spectra from the mixed AnxA6-lipid spectra allowed us to distinguish the characteristic contribution of the protein. One can easily notice that the lipid environment stabilizes the highly α-helical structure of AnxA6 (Fig. 8 *A*, *solid line*), best seen in the case of AnxA6a (Fig. 8 *B*, *solid line*). The amide-I band is very sharp, without a significant contribution of peaks characteristic for β-structures or random coil structures.

The formation of a negative band ~1680 cm^{-1} and the relatively high intensity of amide-II band in comparison with the amide-I band indicates that the orientation of the transition moment of the α-helices is close to 30° with respect to the normal to the interface according to simulated models. The change in orientation is also confirmed by the shift of position of α-helices' maximum in the amide-I band from 1655 to 1651 cm^{-1} (Cornut et al., 1996).

The C-terminal peptide fragment of AnxA6 reveals a significantly different behavior in the membrane-bound form. The interaction of AnxA6b with lipids is weaker

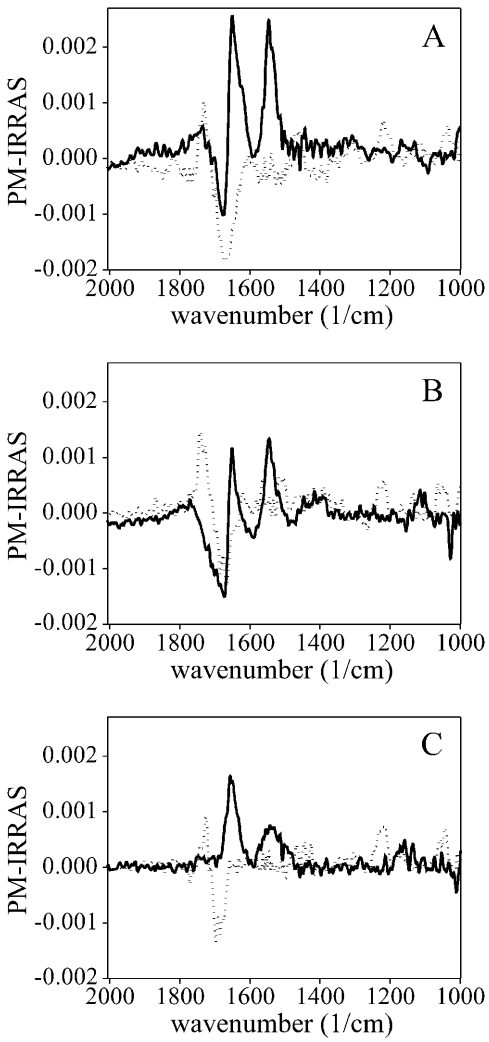

FIGURE 8 PM-IRRAS spectra of AnxA6 (*A*), and the N- (*B*) and C-terminal (*C*) peptide fragments of the protein recorded in the presence of mixed phospholipid film. The concentration of the protein injected into the subphase consisting of 20 mM citrate buffer, pH 5.0, 100 mM NaCl, and 0.1 mM EGTA (*A* and *B*) or 20 mM citrate buffer, pH 5.0, 5 mM NaCl, and 0.1 mM EGTA (*C*), was 300 nM. After stabilization of the lipid/protein monolayers PM-IRRAS spectra were collected. Dotted line represents spectra recorded for pure phospholipid monolayers made of DMPS:DMPE mixed at a weight ratio of 1:1 (corresponding to $\pi = 27$ mN/m). Solid line denotes spectra of protein/phospholipid monolayers after subtraction of the lipid spectra to extract the component characteristic for protein. Non-smoothed spectra typical for at least three independent determinations are shown.

(Fig. 8 *C*, *solid line*), and is strongly inhibited by higher ionic strength (not shown) as used for AnxA6 and its N-terminal fragment (see Fig. 8, *A* and *B*). For this reason, a buffer with low salt content was used. The sharp amide-I band is located ~1655 cm^{-1}. The amide-I/amide-II ratio for AnxA6b amounts to 3, consistent with the orientation of the α-helices parallel to the interface. For comparison, the amide-I/amide-II values obtained for AnxA6, AnxA6a, and AnxA6b are summarized in Table 1.

TABLE 1 The effect of initial surface pressure (π_i) of lipid monolayer on orientation of AnxA6 and its fragments AnxA6a and AnxA6b as indicated by amide-I/amide-II ratio

Protein	π_i	Amide I/Amide II
AnxA6	0 mN/m	1.93:1.96
AnxA6	5 mN/m	1.35:1.39
AnxA6	15 mN/m	0.86:0.88
AnxA6	27 mN/m	0.73:0.75
AnxA6a	0 mN/m	1.98:2.04
AnxA6a	5 mN/m	4.01:4.27
AnxA6a	15 mN/m	1.53:1.57
AnxA6a	27 mN/m	0.72:0.76
AnxA6b	0 mN/m	2.86:3.01
AnxA6b	27 mN/m	2.90:2.97

Influence of condensation of lipid monolayer on protein orientation

To investigate the relationship between phospholipid arrangements and the preferable orientation of the protein in the membrane-bound form, PM-IRRAS spectra at different initial lipid surface pressures were measured. A marked dependence of the peptide orientation on the applied surface pressure was observed for the mixed lipid/AnxA6 and lipid/AnxA6a monolayers (Fig. 9, *A* and *B*). At a low initial pressure of the lipid monolayer the α-helices lie flat on the surface, and the first slight reorientation of AnxA6 (Fig. 9 *A*) or AnxA6a (Fig. 9 *B*) occurs when the lipid monolayer is condensed to 15 mN/m (amide-I/amide-II ratio decreases, Table 1). At higher pressures (27 mN/m), further reorientation takes place and the average orientation of the α-helices amounts to 30° with respect to the normal to the interface. In the case of AnxA6b, no changes in orientation were detected and despite the high pressure of the lipid monolayer the orientation of α-helices remained flat (e.g., 90°, data not shown).

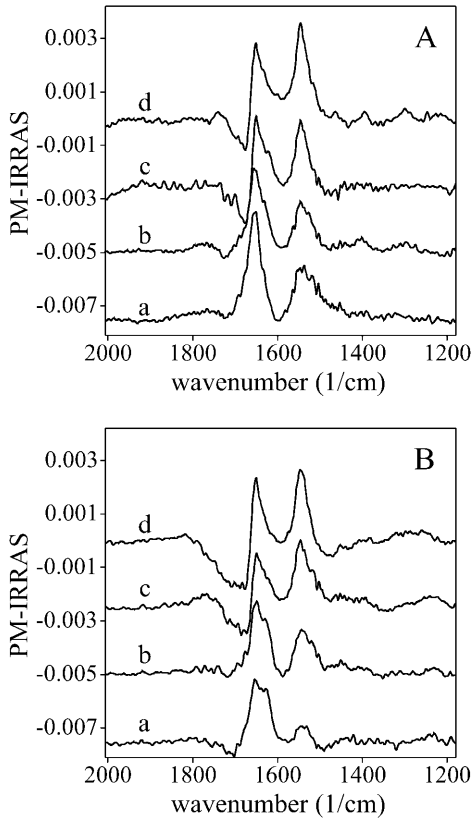

FIGURE 9 The effect of molecular packing of lipid monolayers on AnxA6 (*A*) or AnxA6a (*B*) structure and orientation. PM-IRRAS spectra of AnxA6 or AnxA6a were collected at various initial pressures of the phospholipid monolayer: 0 mN/m (no lipid monolayer), traces *a*; 5 mN/mm, traces *b*; 15 mN/m, traces *c*; and 27 mN/m, traces *d*. In each experiment the same subphase composition, 20 mM citrate buffer, pH 5.0, 100 mM NaCl, and 0.1 mM EGTA, was used. Protein concentration was 300 nM. Phospholipid monolayers were made of DMPS:DMPE at a weight ratio of 1:1. One set of typical spectra from three experiments is shown.

DISCUSSION

Interaction of AnxA6 with membranes at acidic pH is controlled by its N-terminal half

Previous results have revealed that annexins can interact with membranes in a Ca^{2+}-dependent as well as Ca^{2+}-independent manner. Some of them (AnxA5, AnxA6, and AnxB12) may exist in three interchangeable forms—namely, a soluble; one interacting peripherally with the membrane surface; and a transmembrane form similar to other integral membrane proteins. We now report a pH-dependent association of human recombinant AnxA6 with membranes that led to a molecular model of protein insertion in the membrane. The influence of Ca^{2+} and pH on the structure and hydrophobicity of AnxA6 may affect the nature of AnxA6 interactions with membranes. One obvious effect of lowering the pH on AnxA6 is a change of hydrophobicity due to the increasing protonation of Asp and Glu residues which is accompanied by secondary changes consisting in a slight increase of β-sheet and random coil structures. We observed that AnxA6 adsorption at the air-water interface is favored by lowering the pH, consistent with increasing hydrophobicity. PM-IRRAS spectra of AnxA6 at low pH indicated that a substantial amount of α-helix remains in the protein and that most of the α-helices are oriented parallel to the air-water interface. This suggests that although AnxA6 secondary structure is affected by low pH, a relatively large amount of α-helix is preserved and preferentially oriented. Whether such a conformational state may be regarded as a molten globule state remains to be further investigated. Nevertheless, the conformational property, such as preferentially oriented α-helices, may have a functional significance, as it will be discussed below. The β-sheet structures are not well-evidenced in the PM-IRRAS spectra of AnxA6 because we observe a mixed effect evoked on the spectrum by the N- and C-terminal halves of the molecule. These structures are better seen for the N-terminal fragment AnxA6a due to the fact that all pH-induced

structural changes are related mostly to this portion of the molecule. In the case of AnxA6, a strong influence of lipid bilayer on the protein structure was noticed. The presence of a membrane strongly favors reorganization of protein configuration and stabilizes its highly α-helical structure.

Implications for ion channel formation by AnxA6 at low pH

The rearrangements of AnxA6 domains in the presence of lipids are accompanied with a reorientation of the α-helices from a parallel toward a perpendicular orientation, $\sim$60° with respect to the plane of the membrane, as evidenced by the PM-IRRAS spectra of lipid monolayers in the presence of AnxA6. The partial unfolding observed in solution at low pH could be considered as an intermediate state between the soluble and the membrane form of the protein. Our experimental observations support the model of spontaneous, posttranslational membrane insertion of proteins and peptides developed by White et al. (1998, 2001). Acidic pH induced a partially unfolded state of AnxA6 in solution. The binding of AnxA6 to the membrane surface may promote refolding of its secondary structure. Additionally, formation of hydrogen bonds in the polypeptide backbone lowers the free energy of incorporation of a protein into the hydrophobic core of the bilayer (White et al., 2001). Our measurements are consistent with the suggestion that the reorientation of the α-helices of AnxA6 might enhance the protein insertion. Such domain movements could be mediated by the lipid surface. Although infrared spectra may provide information on hydrogen bonds, in the case of PM-IRRAS spectra of AnxA6 the most likely interpretation of the spectral changes is that they are associated with changes in orientation of protein domains. This interpretation is supported by the fact that the N-terminal AnxA6a and the C-terminal AnxA6b behave differently in the presence of lipids, although their secondary structures are almost identical as probed by CD and infrared spectra. Indeed, movements of the α-helical segments in AnxA6a upon lipid compression are similar to those in AnxA6, whereas the α-helical segments in AnxA6b remain parallel to the membrane surface during lipid compression. The ''membrane conformation'' must differ from that observed for the native protein at neutral pH. The findings of Isas et al. (2000, 2003) led to the hypothesis that AnxA6 in an inside-out organization, with exposition of a hydrophobic surface (normally hidden inside the protein molecule), interacts with the acyl segments of phospholipids in the membrane-bound state at low pH. Comparison of the AnxA6 behavior described in this report with that of AnxB12 (Isas et al., 2003) reveals slight differences. The most important one is that AnxB12 conformation seems to be stable upon medium acidification.

CONCLUDING REMARKS

Our findings emphasize that the mechanism of acidic pH-induced ion channel formation by AnxA6 involves at least two steps. The first step is associated with pH-induced changes in hydrophobicity leading to slight conformational changes, and the second one is related to movements of protein domains comprising α-helical segments located mainly in the N-terminal part. Such movements of protein domains are mediated by the interactions with lipids and are not necessarily calcium-dependent. By using proteolytic enzymes, it was demonstrated that AnxA6 and its N-terminal fragment (AnxA6a) are partially protected when interacting with liposomes at low pH, whereas the C-terminal fragment (AnxA6b) was not protected. This suggests that intact AnxA6 under acidic conditions is not completely an integral membrane protein. This is also consistent with the estimated thickness of 26 Å for the AnxA6 protein, corresponding to one layer of AnxA6. ^{125}I-TID labeling indicated that a significant part of AnxA6 is in contact with the hydrophobic region of the membrane whereas the C-terminal part (AnxA6b) seems not to be in contact with the hydrophobic layer. Taken together, our findings are consistent with a topological model of AnxA6 insertion, whereby it is primarily the N-terminal part that is in contact with the lipid hydrophobic region, but the C-terminal region that is in contact with the aqueous medium. Based on the ease of obtaining proteoliposomes formed with AnxA6 at low pH, AnxA6 is probably not an integral transmembrane protein but inserts only partially in the hydrophobic core. This structural feature may have a functional significance, especially with respect to ion conductance properties. In fact, AnxA6 at low pH does not exhibit specific conductance toward any cation (Golczak et al., 2001a), and its ion channel conductance properties indicate pores of variable diameter.

A drop in pH may occur under physiological conditions, especially at the membrane-water interface where the interfacial pH may be quite different from that of bulk medium. A question one may ask is whether the pH is sufficiently low to induce such ion-channel formation and under what conditions one should expect it. One possibility, already suggested by other groups (Arispe et al., 1996; Wang et al., 2003), is that annexins may be involved in ion channel formation within extracellular matrix vesicles.

We thank Professor René Buchet from Université Claude Bernard, Villeurbanne, France, for fruitful discussion, Professor R. Huber from the Max-Planck-Institut fur Biochemie, Martinsried, Germany, for providing cDNA for human AnxA6 (isoform I), and Professor R. Donato from Universita di Perugia, Italy, for sending *E. coli* transformed with AnxA6, AnxA6a, and AnxA6b cDNAs.

This work was supported by grants from the State Committee for Scientific Research (KBN, Poland, grant No. 3 P04A 007 22 to J.B.-P.), and from the Centre National de la Recherche Scientifique (to B.D.). M.G. was recipient of a Marie Curie-Sklodowska fellowship and a scholarship from the Polish Science Foundation.

REFERENCES

Arispe, N., E. Rojas, B. R. Genge, L. N. Y. Wu, and R. E. Wuthier. 1996. Similarity in calcium channel activity of annexin V and matrix vesicles in planar lipid bilayers. *Biophys. J.* 71:1764–1775.

Avila-Sakar, A. J., C. E. Creutz, and R. H. Kretsinger. 1998. Crystal structure of bovine annexin VI in a calcium-bound state. *Biochim. Biophys. Acta.* 1387:103–116.

Avila-Sakar, A. J., R. H. Kretsinger, and C. E. Creutz. 2000. Membrane-bound 3D structures reveal the intrinsic flexibility of annexin VI. *J. Struct. Biol.* 130:54–62.

Bandorowicz-Pikula, J., A. Kirilenko, R. van Deursen, M. Golczak, M. Kuhnel, J. M. Lancelin, S. Pikula, and R. Buchet. 2003. A putative consensus sequence for the nucleotide-binding site of annexin A6. *Biochemistry.* 42:9137–9146.

Benz, J., A. Bergner, A. Hofmann, P. Demange, P. Gottig, S. Liemann, R. Huber, and D. Voges. 1996. The structure of recombinant human annexin VI in crystals and membrane-bound. *J. Mol. Biol.* 260:638–643.

Beermann, B. B., H. J. Hinz, A. Hofmann, and R. Huber. 1998. Acid-induced equilibrium unfolding of annexin V wild type shows two intermediate states. *FEBS Lett.* 423:265–269.

Binder, H., G. Kohler, K. Arnold, and O. Zschornig. 2000. pH- and Ca^{2+}-dependent interaction of annexin V with phospholipid membranes: a combined study using fluorescence techniques, microelectrophoresis and infrared spectroscopy. *Phys. Chem. Chem. Phys.* 2:4615–4623.

Blaudez, D., J. M. Turlet, J. Dufourcq, D. Bard, T. Buffeteau, and B. Desbat. 1996. Investigations at the air-water interface using polarization modulation IR spectroscopy. *J. Chem. Soc. Faraday Trans.* 92:525–530.

Bradford, M. M. 1976. A rapid and sensitive method for the quantitation of microgram quantities of protein utilizing the principle of protein-dye binding. *Anal. Biochem.* 72:248–254.

Buffeteau, T., D. Blaudez, E. Pere, and B. Desbat. 1999. Optical constant determination in the infrared of uniaxially oriented monolayers from transmittance and reflectance measurements. *J. Phys. Chem. B.* 103: 5020–5027.

Burger, A., R. Berendes, D. Voges, R. Huber, and P. Demange. 1993. A rapid and efficient purification method for recombinant annexin V for biophysical studies. *FEBS Lett.* 329:25–28.

Cartailler, J. P., H. T. Haigler, and H. Luecke. 2000. Annexin XII E105K crystal structure: identification of a pH-dependent switch for mutant hexamerization. *Biochemistry.* 39:2475–2483.

Castano, S., D. Blaudez, B. Desbat, J. Dufourcq, and H. Wroblewski. 2002. Secondary structure of spiralin in solution, at the air-water interface, and in interaction with lipid monolayers. *Biochim. Biophys. Acta.* 1562: 45–56.

Chow, A., A. J. Davis, and D. J. Gawler. 2000. Identification of a novel protein complex containing annexin VI, Fyn, Pyk2, and the $p120^{GAP}$ C2 domain. *FEBS Lett.* 469:88–92.

Cornut, I., B. Desbat, J. M. Turlet, and J. Dufourcq. 1996. In situ study by polarization-modulated Fourier transform infrared spectroscopy of the structure and orientation of lipids and amphipathic peptides at the air-water interface. *Biophys. J.* 70:305–312.

Cuervo, A. M., A. V. Gomes, J. A. Barnes, and J. F. Dice. 2000. Selective degradation of annexins by chaperone-mediated autophagy. *J. Biol. Chem.* 275:33329–33335.

de Diego, I., F. Schwartz, H. Siegfried, P. Dauterstedt, J. Heeren, U. Beisiegel, C. Enrich, and T. Grewal. 2002. Cholesterol modulates the membrane binding and intracellular distribution of annexin 6. *J. Biol. Chem.* 277:32187–32194.

Garbuglia, M., M. Verzini, A. Hofmann, R. Huber, and R. Donato. 2000. S100A1 and S100B interactions with annexins. *Biochim. Biophys. Acta.* 1498:192–206.

Gerke, V., and S. E. Moss. 2002. Annexins: from structure to function. *Physiol. Rev.* 82:331–371.

Golczak, M., A. Kicinska, J. Bandorowicz-Pikula, R. Buchet, A. Szewczyk, and S. Pikula. 2001a. Acidic pH-induced folding of annexin VI is a prerequisite for its insertion into lipid bilayers and formation of ion channels by the protein molecules. *FASEB J.* 15:1083–1085.

Golczak, M., A. Kirilenko, J. Bandorowicz-Pikula, and S. Pikula. 2001b. Conformational states of annexin VI in solution induced by acidic pH. *FEBS Lett.* 496:49–54.

Golczak, M., A. Kirilenko, J. Bandorowicz-Pikula, and S. Pikula. 2001c. N- and C-terminal halves of human annexin VI differ in ability to form low pH-induced ion channels. *Biochem. Biophys. Res. Commun.* 284: 785–791.

Grewal, T., J. Heeren, D. Mewawala, T. Schnitgerhans, D. Wendt, G. Salomon, C. Enrich, U. Beisiegel, and S. Jackle. 2000. Annexin VI stimulates endocytosis and is involved in the trafficking of low density lipoprotein to the prelysosomal compartment. *J. Biol. Chem.* 275:33806–33813.

Gu, F., and J. Gruenberg. 2000. ARF1 regulates pH-dependent COP functions in the early endocytic pathway. *J. Biol. Chem.* 275:8154–8160.

Hoppe, J., J. Brunner, and B. B. Jorgensen. 1984. Structure of the membrane-embedded F_0 part of F_1F_0 ATP synthase from *Escherichia coli* as inferred from labeling with 3-(trifluoromethyl)-3-(*m*-[^{125}I]iodophenyl)diazirine. *Biochemistry.* 23:5610–5616.

Isas, J. M., J. P. Cartailler, Y. Sokolov, D. R. Patel, R. Langen, H. Luecke, J. E. Hall, and H. T. Haigler. 2000. Annexins V and XII insert into bilayers at mildly acidic pH and form ion channels. *Biochemistry.* 39:3015–3022.

Isas, J. M., D. R. Patel, C. Jao, S. Jayasinghe, J. P. Cartailler, H. T. Haigler, and R. Langen. 2003. Global structural changes in annexin 12. The roles of phospholipid, Ca^{2+}, and pH. *J. Biol. Chem.* 278:30227–30234.

Ishitsuka, R., K. Kojima, H. Utsumi, H. Ogawa, and I. Matsumoto. 1998. Glycosaminoglycan binding properties of annexin IV, V, and VI. *J. Biol. Chem.* 273:9935–9941.

Jackle, S., U. Beisiegel, F. Rinninger, F. Buck, A. Grigoleit, A. Block, I. Groger, H. Greten, and E. Windler. 1994. Annexin VI, a marker protein of hepatocytic endosomes. *J. Biol. Chem.* 269:1026–1032.

Jost, M., D. Zeuschner, J. Seemann, K. Weber, and V. Gerke. 1997. Identification and characterization of a novel type of annexin-membrane interaction: Ca^{2+} is not required for the association of annexin II with early endosomes. *J. Cell Sci.* 110:221–228.

Kaercher, T., D. Honig, and D. Mobius. 1993–1994. Brewster angle microscopy. A new method of visualizing the spreading of Meibomian lipids. *Int. Ophthalmol.* 17:341–348.

Kirilenko, A., M. Golczak, S. Pikula, R. Buchet, and J. Bandorowicz-Pikula. 2002. GTP-induced membrane binding and ion channel activity of annexin VI: is annexin VI a GTP biosensor? *Biophys. J.* 82:2737–2745.

Kohler, G., U. Hering, O. Zschornig, and K. Arnold. 1997. Annexin V interaction with phosphatidylserine-containing vesicles at low and neutral pH. *Biochemistry.* 36:8189–8194.

Ladokhin, A. S., J. M. Isas, H. T. Haigler, and S. H. White. 2002. Determining the membrane topology of proteins: insertion pathway of a transmembrane helix of annexin 12. *Biochemistry.* 41:13617–13626.

Laemmli, U. K. 1970. Cleavage of structural proteins during the assembly of the head of bacteriophage T4. *Nature* (*Lond.*). 227:680–685.

Lambert, O., N. Cavusoglu, J. Gallay, M. Vincent, J. L. Rigaud, J. P. Henry, and J. Ayala-Sanmartin. 2004. Novel organization and properties of annexin 2-membrane complexes. *J. Biol. Chem.* 279:10872–10882.

Langen, R., J. M. Isas, W. L. Hubbell, and H. T. Haigler. 1998a. A transmembrane form of annexin XII detected by site-directed spin labeling. *Proc. Natl. Acad. Sci. USA.* 95:14060–14065.

Langen, R., J. M. Isas, H. Luecke, H. T. Haigler, and W. L. Hubbell. 1998b. Membrane-mediated assembly of annexins studied by site-directed spin labeling. *J. Biol. Chem.* 273:22453–22457.

Lavoie, H., J. Gallant, M. Grandbois, D. Blaudez, B. Desbat, F. Boucher, and C. Saless. 1999. The behaviour of membrane proteins in monolayers at the gas-water interface: comparison between photosystem II, rhodopsin and bacteriorhodopsin. *Mat. Sci. Eng. C-Bio. S.* 10:147–154.

Luecke, H., B. T. Chang, W. S. Mailliard, D. D. Schlaepfer, and H. T. Haigler. 1995. Crystal structure of the annexin XII hexamer and implications for bilayer insertion. *Nature* (*Lond.*). 378:512–515.

Oling, F., W. Bergsma-Schutter, and A. Brisson. 2001. Trimers, dimers of trimers, and trimers of trimers are common building blocks of annexin A5 two-dimensional crystals. *J. Struct. Biol.* 133:55–63.

Ortega, D., A. Pol, M. Biermer, S. Jackle, and C. Enrich. 1998. Annexin VI defines an apical endocytic compartment in rat liver hepatocytes. *J. Cell Sci.* 111:261–269.

Pikula, S. 2003. Acidic pH-induced ion channels formed by annexin VI—transformation from soluble to membrane integral protein. *In* Annexins: Biological Importance and Annexin-Related Pathologies. J. Bandorowicz-Pikula, editor. Kluwer Academic/Plenum Publishers, New York, NY, and Landes Bioscience, Georgetown, TX. 182–195.

Pol, A., D. Ortega, and C. Enrich. 1997. Identification of cytoskeleton-associated proteins in isolated rat liver endosomes. *Biochem. J.* 327: 741–746.

Pons, M., G. Ihrke, S. Koch, M. Biermer, A. Pol, T. Grewal, S. Jackle, and C. Enrich. 2000. Late endocytic compartments are major sites of annexin VI localization in NRK fibroblasts and polarized WIF-B hepatoma cells. *Exp. Cell Res.* 257:33–47.

Pons, M., T. Grewal, E. Rius, T. Schnitgerhans, S. Jackle, and C. Enrich. 2001a. Evidence for the involvement of annexin 6 in the trafficking between the endocytic compartment and lysosomes. *Exp. Cell Res.* 269:13–22.

Pons, M., F. Tebar, M. Kirchhoff, S. Peiro, I. de Diego, T. Grewal, and C. Enrich. 2001b. Activation of Raf-1 is defective in annexin 6 over-expressing Chinese hamster ovary cells. *FEBS Lett.* 501:69–73.

Reeves, J. P., and R. M. Dowben. 1969. Formation and properties of thin-walled phospholipids vesicles. *J. Cell. Physiol.* 73:49–60.

Risse, T., W. L. Hubbell, J. M. Isas, and H. T. Haigler. 2003. Structure and dynamics of annexin 12 bound to a planar lipid bilayer. *Phys. Rev. Lett.* 91:188101. Epub 2003 Oct 29.

Silvestro, L., and P. H. Axelsen. 1999. Fourier transform infrared linked analysis of conformational changes in annexin V upon membrane binding. *Biochemistry.* 38:113–121.

Sopkova-De Oliveira Santos, J., S. Fischer, C. Guilbert, A. Lewit-Bentley, and J. C. Smith. 2000. Pathway for large-scale conformational change in annexin V. *Biochemistry.* 39:14065–14074.

Towbin, H., T. Staehelin, and J. Gordon. 1979. Electrophoretic transfer of proteins from polyacrylamide gels to nitrocellulose sheets: procedure and some applications. *Proc. Natl. Acad. Sci. USA.* 76:4350–4354.

van Voorst, F., C. van der Does, J. Brunner, A. J. Driessen, and B. de Kruijff. 1998. Translocase-bound SecA is largely shielded from the phospholipid acyl chains. *Biochemistry.* 37:12261–12268.

Wang, W., J. Xu, and T. Kirsch. 2003. Annexin-mediated Ca^{2+} influx regulates growth plate chondrocyte maturation and apoptosis. *J. Biol. Chem.* 278:3762–3769.

White, S. H., W. C. Wimley, A. S. Ladokhin, and K. Hristova. 1998. Protein folding in membranes: determining energetics of peptide-bilayer interactions. *Methods Enzymol.* 295:62–87.

White, S. H., A. S. Ladokhin, S. Jayasinghe, and K. Hristova. 2001. How membranes shape protein structure. *J. Biol. Chem.* 276:32395–32398.

Wu, F., A. Gericke, C. R. Flach, T. R. Mealy, B. A. Seaton, and R. Mendelsohn. 1998. Domain structure and molecular conformation in annexin V/1,2-dimyristoyl-*sn*-glycero-3-phosphate/Ca^{2+} aqueous monolayers: a Brewster angle microscopy/infrared reflection-absorption spectroscopy study. *Biophys. J.* 74:3278–3281.

Zeuschner, D., W. Stoorvogel, and V. Gerke. 2001. Association of annexin 2 with recycling endosomes requires either calcium- or cholesterol-stabilized membrane domains. *Eur. J. Cell Biol.* 80:499–507.